AMERICAN SOCIETY FOR MICROBIOLOGY | Molecular and Cellular Biology®

RESEARCH ARTICLE

Blockade of Metallothioneins 1 and 2 Increases Skeletal Muscle Mass and Strength

Serge Summermatter,[a] Anais Bouzan,[a] Eliane Pierrel,[a] Stefan Melly,[a] Daniela Stauffer,[a] Sabine Gutzwiller,[a] Erin Nolin,[c] Christina Dornelas,[c] Christy Fryer,[c] Juliet Leighton-Davies,[a] David J. Glass,[b] Brigitte Fournier[a]

Musculoskeletal Diseases, Novartis Institutes for Biomedical Research, Novartis Campus, Basel, Switzerland[a]; Musculoskeletal Diseases, Novartis Institutes for Biomedical Research, Cambridge, Massachusetts, USA[b]; Chemical Biology and Therapeutics, Novartis Institutes for Biomedical Research, Cambridge, Massachusetts, USA[c]

ABSTRACT Metallothioneins are proteins that are involved in intracellular zinc storage and transport. Their expression levels have been reported to be elevated in several settings of skeletal muscle atrophy. We therefore investigated the effect of metallothionein blockade on skeletal muscle anabolism *in vitro* and *in vivo*. We found that concomitant abrogation of metallothioneins 1 and 2 results in activation of the Akt pathway and increases in myotube size, in type IIb fiber hypertrophy, and ultimately in muscle strength. Importantly, the beneficial effects of metallothionein blockade on muscle mass and function was also observed in the setting of glucocorticoid addition, which is a strong atrophy-inducing stimulus. Given the blockade of atrophy and the preservation of strength in atrophy-inducing settings, these results suggest that blockade of metallothioneins 1 and 2 constitutes a promising approach for the treatment of conditions which result in muscle atrophy.

KEYWORDS muscle metabolism

Received 27 May 2016 **Returned for modification** 23 June 2016 **Accepted** 2 December 2016

Accepted manuscript posted online 12 December 2016

Citation Summermatter S, Bouzan A, Pierrel E, Melly S, Stauffer D, Gutzwiller S, Nolin E, Dornelas C, Fryer C, Leighton-Davies J, Glass DJ, Fournier B. 2017. Blockade of metallothioneins 1 and 2 increases skeletal muscle mass and strength. Mol Cell Biol 37:e00305-16. https://doi.org/10.1128/MCB.00305-16.

Address correspondence to Brigitte Fournier, brigitte.fournier@novartis.com.

Skeletal muscle hypertrophy is characterized in the adult mammal by an increase in the size of preexisting myofibers. The induction of hypertrophy involves an activation of the pathways that increase protein synthesis and inhibition of cellular signaling, which induces protein degradation. Hypertrophy can be induced by the activation of Akt, through multiple potential inputs (1). Akt induces hypertrophy in part by activating the mTOR/70S6 kinase pathway. In addition, Akt inhibits protein degradation, by phosphorylating and therefore blocking Foxo1 and Foxo3—transcription factors which are required for the upregulation of the E3 ubiquitin ligases MuRF1 and MAFbx, which help mediate protein turnover during muscle atrophy (2–4). Therefore, activation of Akt constitutes a critical signaling node to increase muscle hypertrophy and block muscle atrophy (1).

Mammalian metallothioneins (MTs) belong to a family of cysteine-rich, metal-binding proteins. In rodents, four MT isoforms have been identified: the two major isoforms, MT-1 and MT-2, are ubiquitously expressed, while MT-3 and MT-4 show tissue specific expression in the central nervous system and squamous epithelia, respectively. In humans, multiple isoforms have been reported for MT-1 (MT-1A, MT-1B, MT-1E, MT-1F, MT-1G, MT-1H, MT-1M, and MT-1X), while no splice variants are documented for MT-2, MT-3, or MT-4 (5; for a review, see reference 6).

MTs play a role in cellular zinc homeostasis, mitochondrial function (7), defense against oxidative stress (8), and defense against inflammation (5). Moreover, several reports and a recent review highlight a role of metallothioneins in cancer (9), aging (10), and the onset of particular central nervous system diseases (11).

Interestingly, increased levels of metallothioneins in models of rodent and human skeletal muscle atrophy have been reported (12–14). This increase of metallothionein was originally interpreted as a response to oxidative stress. Silencing of metallothionein in muscle myotubes *in vitro* was, however, not associated with changes in oxidative activity (15). A separate *in vivo* study examined the effect of metallothionein deficiency after acute spinal cord injury and concluded that the absence of metallothionein neither exacerbates an oxidative stress response nor impacts muscle atrophy (16). These findings suggest that modulation of metallothionein in atrophy models does not play a major role in the oxidative status of the muscle, or in the mechanism inducing the atrophic process.

Another important function of metallothioneins is to act as a zinc buffering protein. Depending on the redox state of their environment, MTs form either the oxidized protein thionin or the apoprotein thionein. Formation of thionin results from oxidation of zinc-bound metallothionein, linking the redox state of the cells to zinc homeostasis (17). Metallothioneins act in concert with zinc transporters from the SLC39 family (ZIP) involved in zinc uptake and from the SLC30 (ZnT) family responsible for zinc transport into organelles or out of cells (6, 18). Free zinc ions are thought to serve as signaling ions (19); several studies indicate that free zinc activates different pathways and can modulate the insulin and mTOR pathways (20, 21). Changes in free zinc also impact enzymatic activities as shown, for example, for protein tyrosine phosphatase (22). Moreover, changes in subcellular distribution of zinc and generation of free zinc in cells play a role in development of diseases such as type II diabetes (23), cancer (24), and immune diseases (25). Previous studies demonstrated the lack of impact of MT silencing on oxidative state of skeletal muscle cells both *in vitro* and *in vivo* (15, 16). We therefore asked whether MTs could have a role in skeletal muscle metabolism related to its ability to modify intracellular zinc level. In this study, we examined the role of metallothioneins in skeletal muscle cells *in vitro* and *in vivo* to better understand the function of MT-1 and -2 under both normal and atrophic conditions.

RESULTS

Metallothioneins 1 and 2 are upregulated in rodent sarcopenia. We first monitored the gene expression profile of MTs during rodent sarcopenia (the loss of muscle mass and function associated with advanced age [26]). MT-1 and MT-2 mRNA levels in skeletal muscle increased with age (Fig. 1A). As MTs play a role in zinc metabolism, we asked whether zinc levels in muscle were altered in aged animals. Interestingly, we found that total zinc was significantly increased in the gastrocnemius from sarcopenic animals, in comparison to younger controls (Fig. 1B). Interestingly, as shown in Fig. 1C, zinc is capable of regulating MT expression. Therefore, the increase in metallothionein mRNA levels in sarcopenic muscle could be a consequence of the increased total zinc levels. Previously, zinc concentration has been reported to increase in skeletal muscle of tumor-bearing mice, and zinc chelation attenuated muscle wasting (27). Taken together, these data and our observation suggested that zinc concentration in skeletal muscle may play a role in regulating muscle atrophy.

Silencing of metallothioneins 1 and 2 activates the Akt/mTOR pathway and increases myotube size in human skeletal myotubes *in vitro*. Since metallothioneins are important zinc buffering proteins in cells (28), we speculated that silencing of MT-1 and -2 in human myotubes could free intracellular zinc. Free zinc has been reported to activate distinct signaling pathways, including the IGF1 and mTOR pathways (21). We thus assessed Akt, glycogen synthase kinase 3β (GSK3β), and S6RP phosphorylation in myotubes exposed to zinc pyrithione. As shown in Fig. 2A, Akt phosphorylation was strongly induced, with a maximal effect after 2 h, while GSK3β phosphorylation peaked after 2 h and declined thereafter. S6 ribosomal pathway phosphorylation, which is downstream of mTOR/p70S6K signaling, peaked after 6 h (Fig. 2A).

We then asked if changes in MT silencing could induce Akt/mTOR pathway activation, as seen after treatment with zinc pyrithione. As shown in Fig. 2B, when both MT-1 and MT-2 are silenced, MT-1mRNA is decreased by 84% and MT-2 mRNA by 91%.

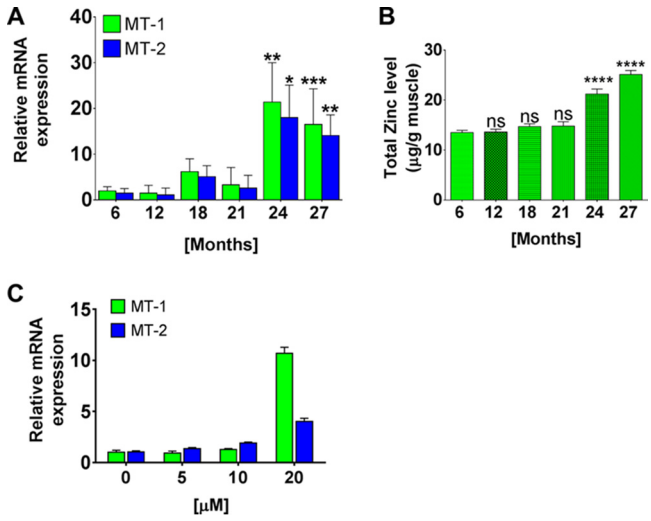

FIG 1 Metallothionein-1 and -2 expression and total zinc are increased in sarcopenic muscle. (A) Increase expression of MT-1 and -2 in sarcopenia. Relative mRNA levels of MT-1 and MT-2 in gastrocnemius of rats aged from 6 to 27 months were assessed by RT-PCR. Values are expressed as means ± SEMs for 8 to 10 mice. Statistical analysis was performed using ANOVA plus the Bonferroni test. *, $P < 0.05$; **, $P < 0.01$; ***, $P < 0.001$ versus 6 months for 24 months and 27 months. (B) Increase in total zinc level in gastrocnemius muscle of rats with sarcopenia. Total zinc was measured in gastrocnemius of rats aged 6 to 27 months as indicated in Materials and Methods. All values are expressed as means ± SEMs for 10 to 12 mice. Statistical analysis was performed by unpaired *t* test. ****, $P < 0.0001$. ns, not significant. (C) Zinc modulates MT-1 and -2 mRNA expression in human myotubes. Human myotubes were treated with increasing doses of zinc sulfate ($ZnSO_4$), as indicated, for 24 h. MT-1 and MT-2 mRNA expression levels were monitored using real-time PCR as indicated in Materials and Methods. Data are expressed as relative mRNA expression ($n = 2$). Statistical analysis was performed using two-way ANOVA. ***, $P < 0.001$; ****, $P < 0.0001$.

Silencing of MT-1 and -2, as shown in Fig. 2B, resulted in activation of the Akt/mTOR pathway as demonstrated by an increase in Akt, GSK3β, and S6RP phosphorylation (Fig. 2C). It is noteworthy that silencing of MT-1 or MT-2 alone was found to be sufficient to increase Akt, GSK3β, and S6RP phosphorylation, although to a smaller extent than concomitant inhibition of the two MTs (data not shown). Consequently, inhibition of both MT-1 and -2 was used for all subsequent experiments.

Activation of the Akt pathway is well documented as being sufficient to trigger myotube and skeletal hypertrophy (4, 29). We therefore silenced MT-1 and -2 using small interfering RNA (siRNA) and found that the absence of metallothionein induced a significant increase in myotube size in naive cells (Fig. 2D). Furthermore, myotubes treated with the atrophy-inducing agent dexamethasone (DEX) were relatively protected from atrophy (Fig. 2D) upon MT blockade. To demonstrate that this increase in myotube size resulted from the activation of the Akt pathway, cells were treated with a specific Akt inhibitor, API-2. We show that inhibition of the Akt pathway abrogates the increase in myotube size observed after silencing of MT-1 and MT-2 (Fig. 2E).

Taken together, these findings provide evidence that MT downregulation has a positive effect on muscle cell anabolism and suggest that the atrophy-induced increase in MT expression contributes to the atrophic phenotype.

Loss of metallothioneins 1 and 2 promotes muscle hypertrophy *in vivo*. We next evaluated the effect of genetic deletion of both metallothioneins 1 and 2 on skeletal muscle *in vivo*. MT-1 and MT-2 knockouts (KOs) were previously generated (30). These mice are deficient for both metallothioneins 1 and 2 proteins and therefore referred to as MT-null mice. MT-null mice demonstrated elevated body weight and a lean body mass (Fig. 3) consistent with published data from another MT-1/MT-2 KO mouse model (31, 32). In addition, we monitored relative increases in the weights of plantaris muscle (+14%; $P < 0.05$), extensor digitorum longus (+30%; $P < 0.05$), tibialis (+20%; $P < 0.001$), and quadriceps (+17%; $P < 0.001$) compared to those in wild-type controls

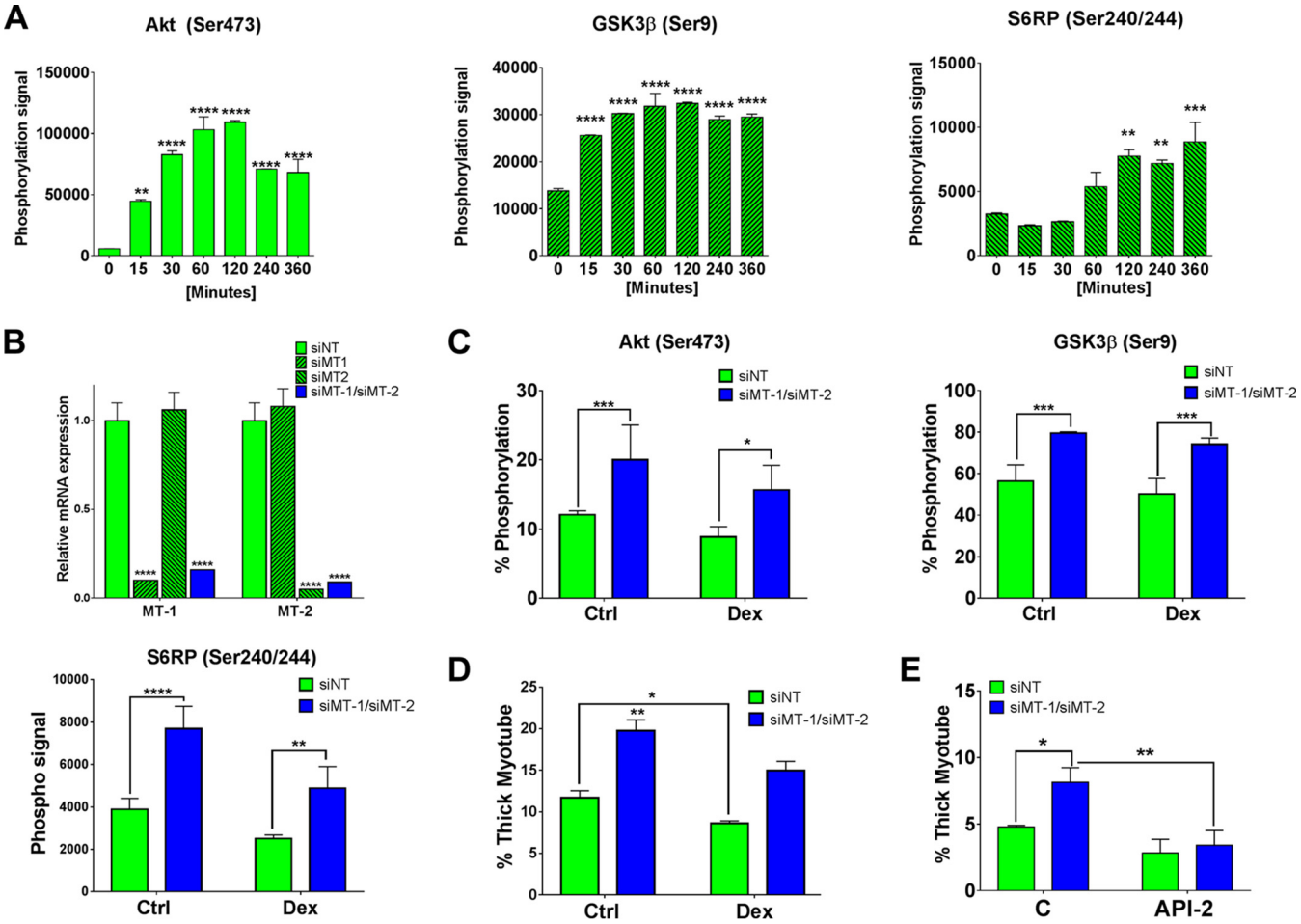

FIG 2 MT-1 and MT-2 silencing increases the Akt pathway activity and myotube diameter in human skeletal muscle cells. (A) Zinc pyrithione triggers the Akt/TOR pathway in human skeletal myotubes. The kinetics of phosphorylation for Akt, GSK3β, and S6RP after treatment of myotubes with 0.5 μM zinc pyrithione was monitored using MSD technology as described in Materials and Methods. Values are expressed as means ± SEMs ($n = 2$) of the phosphorylation signal; statistical analysis was performed using one-way ANOVA. **, $P < 0.01$; ***, $P < 0.001$; ****, $P < 0.0001$. (B) Silencing of MT-1 and MT-2 in human skeletal muscle myotubes. Human skeletal cells were transfected with control siNT (nontarget), with siMT-1 or siMT-2 alone, or with both siMT-1 and MT-2 for 24 h. Values are expressed as relative mRNA expression. Relative levels were calculated by giving an arbitrary value of 100% to the nontarget control. (C) MT-1 and -2 silencing triggers the Akt/TOR pathway in human skeletal myotubes. Myotubes were subjected to a control siRNA or siRNA to MT-1 and MT-2 and treated with a vehicle or 10 μM dexamethasone for 24 h. Phosphorylation of Akt, GSK3β, and S6RP was monitored as indicated using MSD technology as described in Materials and Methods. Values are expressed as mean percentage of phosphorylation signal over expression of total Akt and GSK3β, except for S6RP values, expressed as means ± SEMs ($n = 3$) of the phosphorylation signal. Statistical analysis was performed using two-way ANOVA with *post hoc* Dunnett test. *, $P < 0.05$; **, $P < 0.01$. (D) *In vitro* MT-1 and MT-2 silencing increases the Akt pathway leading to increased myotube size. Myotubes were subjected to a control siRNA or siRNA to MT-1 and MT-2 and treated with a vehicle or 10 μM dexamethasone for 24 h. Values are expressed as means ± SEMs of thick-myotube percentage ($n = 2$). Statistical analysis was performed using two-way ANOVA with *post hoc* Dunnett test. *, $P < 0.05$; **, $P < 0.01$; ***, $P < 0.001$. (E) Increase in myotube size after MT-1 and MT-2 silencing is Akt dependent. Myotubes were transfected with a control siRNA (siRNA NT) or siRNA to MT-1 and MT-2 for 24 h and treated with a vehicle or 25 μM API-2 (Akt inhibitor) for another 24 h. Values are expressed as means ± SEMs of thick-myotube percentage ($n = 2$). Statistical analysis was performed using two-way ANOVA with *post hoc* Dunnett test. *, $P < 0.05$; **, $P < 0.01$.

(Fig. 4A). In contrast, the weight of soleus and gastrocnemius did not reach statistical significance, though there is a clear trend toward hypertrophy (Fig. 4A). Thus, muscles with higher proportions in fast-twitch fibers seemingly exhibited a more pronounced muscle hypertrophy, suggesting that loss of metallothioneins might have a relative greater effect on fast twitch fibers. Indeed, fast-twitch IIb fibers of tibialis anterior showed marked hypertrophy in MT-null animals (Fig. 4B), whereas no changes in diameter of IIa or I/IIx fibers were observed (data not shown). To assess the functional consequences of this type IIb fiber hypertrophy, force-frequency relationships were established *in vivo*. MT-null mice generated significantly higher force at high-frequency stimulation than control animals (Fig. 4C). These data demonstrate that loss of metallothioneins increases muscle mass by preferentially causing hypertrophy of type IIb fibers and that such hypertrophy results in increased muscle strength.

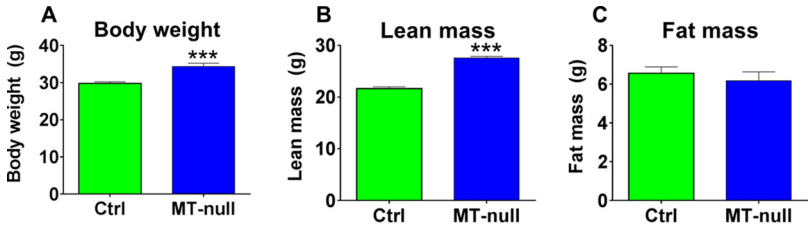

FIG 3 Body weight (A), lean mass (B), and fat mass (C) in control and MT-null mice. All values are expressed as means ± SEs for 13 mice. Statistical analyses were performed by unpaired *t* test. ***, $P < 0.001$.

Expression analyses reveal markers of enhanced muscle growth in MT-null mice. To gain further insights into the molecular mechanisms that drive muscle hypertrophy in MT-null mice, microarray analyses were performed and the results validated by real-time PCR (RT-PCR) (Fig. 5A). Intriguingly, relative mRNA levels of several factors associated with muscle anabolism, notably IGF1 and androgen receptor (AR) (33, 34), were increased in MT-null mice. In addition, the mRNA levels of myogenin and ornithine decarboxylase (Odc1), which has previously been shown to regulate myoblast proliferation (35), were significantly elevated in the absence of metallothioneins. We also found that ablation of metallothioneins increased the mRNA levels of spermine oxidase (Smox). A role for Smox in maintaining basal skeletal muscle gene expression and fiber size has recently been described, and Smox is strongly repressed under muscle catabolic conditions such as fasting, immobilization, and denervation (36). In contrast, forced overexpression of Smox partially prevented muscle fiber

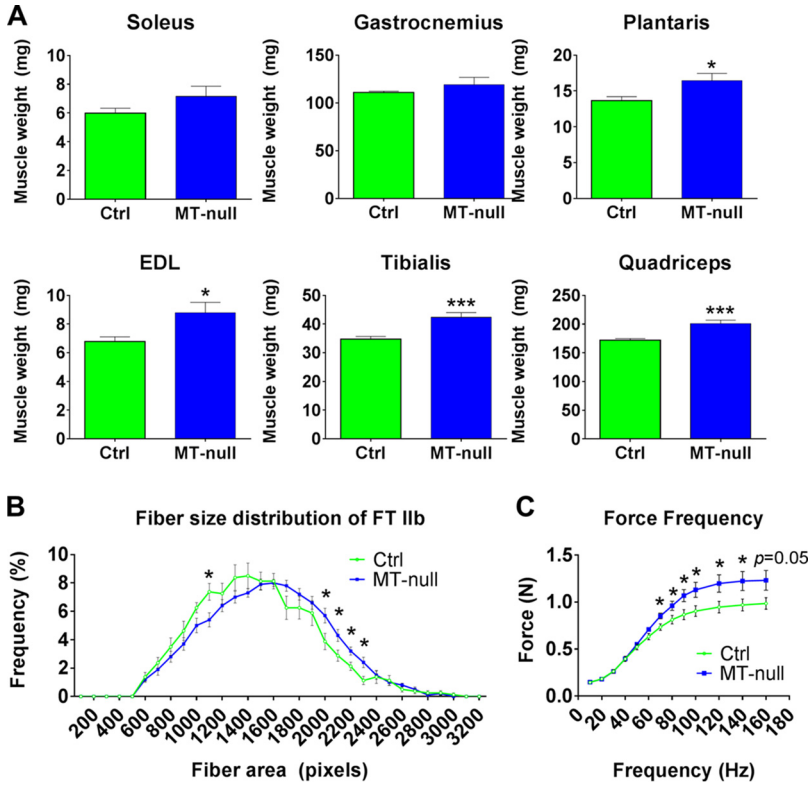

FIG 4 Blockade of MT-1 and -2 increases muscle mass and function. (A) Increased muscle weight in various muscles of MT-null mice. (B) Fiber size distribution showing hypertrophy of type IIb fibers in anterior tibialis. (C) Force-frequency relationship in control and MT-null mice upon evoked hind limb stimulation. All values are expressed as means ± SEs for 8 to 13 mice. Statistical analyses were performed by unpaired *t* test. *, $P < 0.05$; ***, $P < 0.001$.

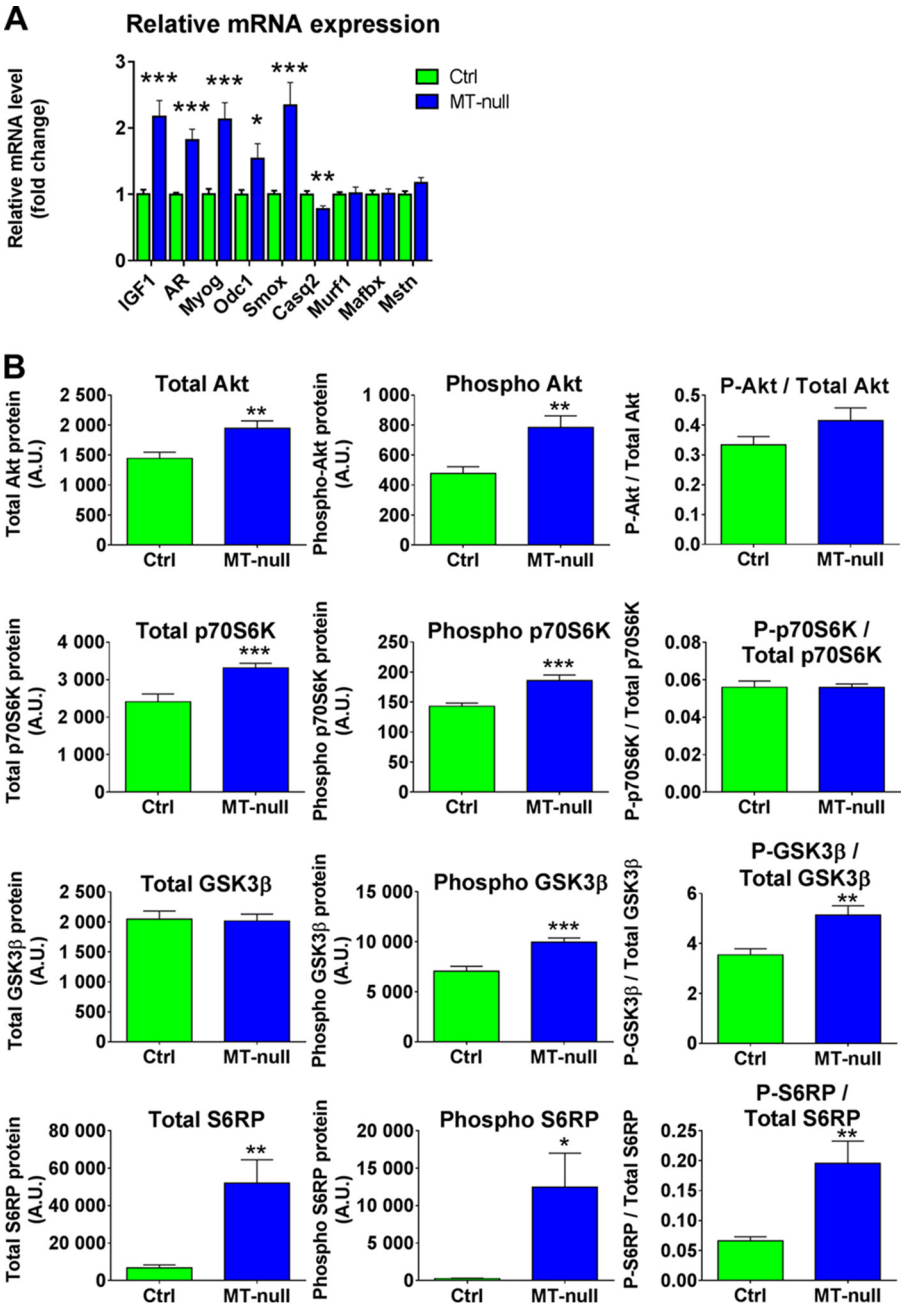

FIG 5 The Akt pathway is activated in skeletal muscle of MT-null mice. (A) Relative mRNA levels of genes regulated in MT-deficient mice as assessed by RT-PCR. (B) Total and phosphorylated protein expression as well as ratios of Akt, GSK3β, p70S6K, and S6RP in control and MT-null mice. All values are expressed as means ± SEs for 13 mice. Statistical analyses were performed by unpaired *t* test. *, $P < 0.05$; **, $P < 0.01$; ***, $P < 0.001$.

atrophy under these conditions (36). Finally, reduced mRNA levels of calsequestrin 2 (Casq2), a marker of slow-twitch muscles, were found in the absence of metallothioneins 1 and 2 (Fig. 5A). Relative mRNA levels of genes involved in protein degradation or growth inhibition, such as the genes for Murf, Mafbx, and myostatin, were, however, not altered in these animals (Fig. 5A). Hence, the transcriptional profiling of skeletal muscle of MT-null mice further corroborates a role for metallothioneins in regulating skeletal muscle mass.

Loss of metallothioneins 1 and 2 increases the activity of anabolic pathways in skeletal muscle. Since we have found that MT silencing resulted in activation of the

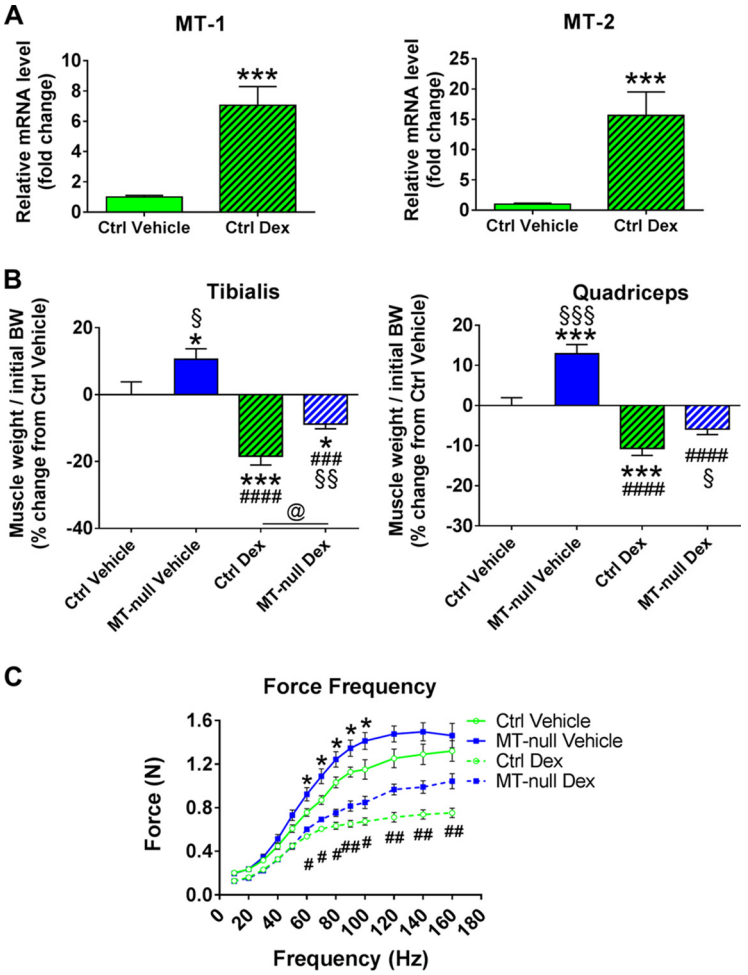

FIG 6 Metallothioneins blockade counters glucocorticoid-induced atrophy and loss of muscle strength. (A) Relative mRNA levels of metallothioneins 1 and 2 in skeletal muscle upon chronic dexamethasone (Dex) administration. (B) Spared muscle weight loss of tibialis and quadriceps in MT-null mice after 14 days of dexamethasone administration. (C) Force-frequency relationship in control and MT-null mice receiving a vehicle or dexamethasone in their drinking water. Values are expressed as means ± SEs for 9 mice. Statistical analyses were performed by ANOVA and Holm-Sidak's *post hoc* test. *, $P < 0.05$; **, $P < 0.01$; ***, $P < 0.001$; ****, $P < 0.0001$ (versus control [Ctrl] vehicle). #, $P < 0.05$; ##, $P < 0.01$; ###, $P < 0.001$; ####, $P < 0.0001$ (versus MT-null vehicle). @, $P < 0.05$ (MT-null Dex versus Ctrl Dex). §, $P < 0.05$; §§, $P < 0.01$ (by unpaired *t* test) (Ctrl versus DEX). For the force-frequency curves, only Ctrl versus KO mice were statistically analyzed by unpaired *t* test. *, $P < 0.05$ (Ctrl vehicle versus MT-null vehicle) #, $P < 0.05$; ##, $P < 0.01$ (Ctrl Dex versus MT-null Dex).

Akt pathway *in vitro* (Fig. 1), we wanted to determine whether MT blockade similarly affects Akt pathway activation *in vivo*. In line with our *in vitro* findings, Akt, GSK3β, p70S6K, and S6RP phosphorylation, reflecting enzymatically active proteins, was elevated in MT-null mice, indicating that metallothionein ablation results in activation of the Akt signaling pathway (Fig. 5B). Our results thus provide a novel link between metallothioneins and Akt pathway activation in skeletal muscle. The finding of Akt activation upon deletion of the MTs is sufficient to explain the hypertrophy and the block of atrophy; the microarray finding that deletion increases IGF1 and AR provides mechanisms for that activation, since both of them increase Akt (1).

Metallothionein deficiency protects from glucocorticoid-induced atrophy. Glucocorticoids are known to provoke marked muscle atrophy in fast-twitch muscles (37). We next assessed whether DEX increases metallothionein mRNA expression in skeletal muscle and indeed found strong upregulation of metallothioneins 1 and 2 (Fig. 6A). We therefore asked whether ablation of metallothionein might in return protect from

muscle atrophy. Moreover, we wanted to determine whether the anabolic effect observed upon metallothionein blockade is preserved upon DEX-induced muscle atrophy.

In tibialis anterior and quadriceps, DEX caused muscle weight losses of 18% and 11%, respectively (Fig. 6B). Intriguingly, MT-null mice maintained higher muscle mass than control animals upon DEX administration, indicating that the muscle-anabolic effect driven by metallothionein deficiency is preserved in the presence of dexamethasone. Consistently, blockade of metallothionein increased muscle strength in spite of the presence of the catabolic stimulus (Fig. 6C). Collectively, our results thus suggest that metallothioneins constitute an attractive target to treat muscle atrophy and counter the loss of muscle strength even in skeletal muscle undergoing protein catabolism.

DISCUSSION

Skeletal muscle atrophy and the resultant weakness it causes are important clinical consequences of cachexia, seen in settings of cancer, renal disease, congestive heart disease, and liver failure (1). It was noted some time ago that metallothioneins 1 and 2 were upregulated dramatically in settings of muscle atrophy, but it was not clear if this was cause or effect—or whether counterregulating this perturbation would be beneficial (12).

Interestingly, increased expression of metallothioneins has been found in several distinct models of rodent and human muscle atrophy (12–14).

In the present study, we have investigated the role of metallothionein *in vitro* in human skeletal muscle cells and *in vivo* in MT-null (metallothionein 1 and 2 loss-of-function) mice in healthy and diseased conditions.

To investigate the mechanism of action of metallothioneins in muscle cells, we used human skeletal muscle cells, which were then differentiated into myotubes. MT-1 and -2 were downregulated using siRNA, resulting in an increase in Akt/mTOR pathway activity. Moreover, we could recapitulate the increase in the Akt/mTOR pathway by transiently increasing free zinc using zinc pyrithione, as reported earlier for nonmuscle cells (21). As reviewed in reference 1, the Akt pathway is responsible for muscle hypertrophy and a blockade of muscle atrophy; consistent with that, we showed that blockade of MT-1 and -2 was associated with Akt pathway activation and an increase in myotube fiber size, both *in vitro* and *in vivo* (Fig. 2E and 4B). The silencing of metallothioneins 1 and 2, potentially by modifying the zinc subcellular distribution, was sufficient to counteract dexamethasone-induced atrophy, consistent with Akt's ability to block the E3 ligases which are upregulated by glucocorticoids (12, 38).

An *in vivo* analysis demonstrated that metallothionein expression and total zinc levels are increased coincident with age-related skeletal muscle loss, also known as sarcopenia (26), suggesting that metallothionein expression, zinc levels, and the muscle loss which is observed as a consequence of old age may be causally related. Questions that remain to be answered in future studies include the determination of the mechanism underlying the increase in total zinc found in sarcopenia and the determination of the concentration of freely available zinc; in this study, we have shown that the increase in total zinc is not due to MTs, since total zinc levels were unchanged in the MT null animals (Fig. 7).

In line with our *in vitro* data, we also found that blockade of metallothioneins 1 and 2 is sufficient to promote muscle hypertrophy *in vivo*. There was a preferential increase in type IIb fibers. This particular finding is clinically relevant, since type IIb fibers are predominant in muscles that are required for strength. Intriguingly, IIb fibers are more prone to atrophy than type IIa or type I fibers (39). Interventions aimed at specifically pomoting maintenance of type IIb fibers would consequently be beneficial in any setting of muscle wasting. Importantly, we now provide strong evidence that muscle hypertrophy upon metallothionein ablation is accompanied by increased muscle strength, and that interventions targeting metallothioneins hence concomitantly increase muscle mass and improve muscle function.

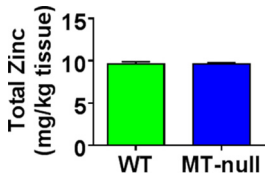

FIG 7 Total zinc levels in gastrocnemius from MT-null mice are unchanged. Total zinc was measured in gastrocnemius of control and MT-null mice as indicated in Materials and Methods. Data are expressed as milligrams of total zinc per kilogram of tissue for 13 mice. Statistical analysis was performed using unpaired *t* test. No difference was detected.

Taken together, our results demonstrate a previously undiscovered role of metallothioneins in the regulation of skeletal muscle mass and function and provide insights into the mechanisms by which metallothioneins increase muscle mass and function in health and disease.

MATERIALS AND METHODS

Cell lines and siRNA-mediated gene silencing. Human skeletal muscle cells were obtained from Cook Myosite (PA). Briefly, the cells were maintained in MyoTonic basal medium (Cook Myosite) supplemented with MyoTonic growth supplement (Cook Myosite), 20% fetal bovine serum (FBS; Gibco), and 0.1% gentamicin (Gibco). Myoblasts were differentiated 24 h after seeding (on collagen-coated plates) by changing to MyoTonic differentiation medium (Cook Myosite) supplemented with 1% FBS, 2% horse serum (Gibco), and 0.1% gentamcin. The cells were differentiated for 5 days. Differentiated myotubes were transfected with 20 nM siRNA (control nontarget, negative AllStars; Hs_MT1a and HS_MT2a; Qiagen) using Dharmafect (ThermoScientific) and subsequently treated with compounds as described in the figure legends.

For gene expression analysis, cells were collected 48 h posttransfection. Cells were collected in 350 μl of RLT lysis buffer from an RNeasy minikit (Qiagen; catalog no. 74106). After siRNA transfection for 24 h, medium was change to starvation medium, 0.02% bovine serum albumin (BSA), for 4 h, and treatment was added for 24 h (RNA; MSD) or 48 h (myotube size; Western blot).

Akt/mTOR pathway analysis in human skeletal muscle myotubes and in muscle. For study of the Akt/mTOR pathway in human skeletal myotubes, cells were plated onto six-well plates at a density of 4.5×10^5 and cultured. Cells were washed in phosphate-buffered saline (PBS), and whole-cell lysate was prepared by following the kit procedure (MSD; K15177D-1). Quantitative determination of total and phosphorylated Akt, GSK3β, p70S6K, and S6RP was performed according to the manufacturer's instructions using an assay kit from MesoScale Discovery using a MesoScale Discovery reader. We used the Akt signaling panel II (phosphoprotein) whole-cell lysate kit (MSD; K15177D-1) and the phospho-S6RP (Ser240/244) assay (MSD; K15139D-1). For muscle, lysis buffer consisting of extraction reagent (Phosphosafe; Novagen Inc., Madison, WI) supplemented with 1% protease inhibitor cocktail (Roche) was added to frozen muscles and muscles were homogenized using a Precellys FastPrep-Machine FP20. Homogenates were centrifuged for 20 min at 4°C (14,000 rpm), and supernatants were collected. For both cell and muscle extract, protein contents were measured with a commercial kit (bicinchoninic acid [BCA] kit; Thermo Scientific). Data are expressed as indicated in the legends for Fig. 2C and 5B.

Myotube size determination. To assess the size of mature human skeletal muscle cell myotubes, cells were fixed with 4% paraformaldehyde for 15 min at room temperature. The cells were then permeabilized with 0.5% Triton and blocked with 10% goat serum (16210; Gibco). Immunostaining was performed with anti-myosin heavy chain (anti-MyHC) antibody (Millipore; 05-716) diluted in 1.5% goat serum-PBS and subsequently with Alexa Fluor 488 (Invitrogen; A11017) and diaminopimelic acid (DAPI) diluted in 1.5% goat serum-PBS. Myotube size was determined using a Cell Insight HCS reader (Thermo Fisher Scientific) and the Morphology protocol from the Cellomics software.

Gene expression profiling. Total RNA was extracted from skeletal muscle using TRIzol reagent (Invitrogen). Reverse transcription was performed with random hexamers on 1 μg of total RNA using a high-capacity reverse transcription kit (Applied Biosystems), and the reaction mixture was diluted 100 times. RT-PCRs were performed in duplicates in 384-well plates on an AB7900HT cycler (Applied Biosystems) using specific TaqMan probes (Applied Biosystems). Data were normalized to two housekeeping genes using the $\Delta\Delta C_T$ threshold cycle (C_T) method. All results are expressed as fold changes over controls. Fluorescence was measured at the end of each cycle, and after 40 reaction cycles, a profile of fluorescence versus cycle number was obtained. Automatic settings were used in most cases to determine the C_T. The comparative method using $2^{-\Delta\Delta CT}$ was used to determine the relative expression; two housekeeping genes were used for normalization (40). All results are expressed as fold changes over controls.

Animals. MT-null mice (129S7/SvEvBrd-Mt1^{tm1Bri} Mt2$^{tm1Bri/J}$) and control animals were obtained from Jackson laboratory. MT-null mice were originally generated in the laboratories of Richard Palmiter at the University of Washington and Ralph Brinster at the University of Pennsylvania by inserting translation stop codons into the metallothionein 1 and 2 genes (30). As a consequence, the two target genes can be transcribed, but will not be translated, resulting in metallothionein 1 and 2 protein deficiency (30).

Mice were maintained in a conventional facility with a fixed 12-h light/dark cycle on a commercial pelleted chow diet containing 18.2% protein and 3.0% fat with an energy content of 15.8 MJ/kg (NAFAG 3890; Kliba, Basel, Switzerland). Food and water were provided *ad libitum*. Adult male MT-null mice and control animals at 17 weeks of age were used for experiments. All studies described in this article were performed according to criteria outlined for the care and use of laboratory animals and with approval of the veterinary office of the canton Basel, Switzerland.

Dexamethasone-induced atrophy model. To induce muscle atrophy, dexamethasone (Sigma) was administered in the drinking water at a dose of 1.25 mg/kg/day for 14 days. Since administration of dexamethasone causes an increase in water consumption, the concentration of dexamethasone was adjusted periodically in order to maintain the dose at 1.25 mg/kg/day. Force-frequency was measured after 14 days, and animals were then euthanized to assess the degree of muscle atrophy.

Determination of total zinc in muscle. Determination of total zinc was performed using inductively coupled plasma optical emission spectrometry (ICP-OES) (41). Data are expressed as micrograms of total zinc per milligram of muscle tissue.

Fiber diameter analysis. Ten-micrometer-thick serial sections of frozen tibialis anterior were cut in a cryostat. For immunohistochemical detection of laminin to outline the sarcolemma, cryosections were permeabilized with 0.5% Triton X-100 and blocked in 2% goat serum. Sections were incubated for 5 min in 5% H_2O_2 and then with a rabbit polyclonal antibody against laminin and monoclonal antibodies against type IIa (1:200) or type IIb (1:100) fibers overnight at 4°C. After being washed in PBS three times for 10 min each time, sections were incubated with Alexa Fluor 488–anti-rabbit secondary antibody (1:100; Invitrogen) for 1 h at 25°C, followed by three washes in PBS to detect laminin. Sections were then incubated with secondary antibody with Alexa Fluor 350 or Alexa Fluor 555 (both at 1:200 for 1 h at 25°C) to reveal type IIa and IIb fibers, respectively, followed by three washes in PBS. Unstained fibers were classified as type I/IIx. Slides were mounted with ProLong Gold antifade reagent (Invitrogen). Images of the entire tissue section were acquired using an Olympus scan VS120 microscope (Olympus Corporation), and the cross-sectional area of the individual fibers in the section was measured automatically using Robias Astoria (v.4.1) software. The means of the fiber cross-sectional areas in each muscle section were determined, and the frequency distributions of the fiber cross-sectional area were plotted.

Force-frequency relationship. Evoked force was measured noninvasively via electrical stimulation of the hind leg through transcutaneous electrodes. After the animals were anesthetized, the evoked muscle contraction was recorded on a homemade pedal (force transducer) connected to the foot of the animal and allowing recording the pressure of the foot upon stimulation. Various frequencies ranging from 10 to 160 Hz were sequentially applied and tetanic forces recorded at each frequency.

Statistical analysis. Statistical analyses were performed using Prism 6 (GraphPad Software, Inc., La Jolla, CA) or SPSS (IBM, Armonk, NY). Tests used for the experiments were the *t* test and one- or two-way analysis of variance (ANOVA), with *post hoc* tests as indicated. Values are expressed as means ± standard errors of the means (SEMs). Differences were considered to be significant when the probability value was <0.05.

ACKNOWLEDGMENTS

We are grateful to Michaela Kneissel and Estelle Trifilieff for their continuous support during the course of this study. We thank W. Maret (King's College London, UK) for very useful discussion. We are indebted to Laurent Gelman (Friedrich Miescher Institute) and Amy Palmer (University of Colorado) for stimulating discussions. We thank Anne-Ulrike Trendelenburg, Sophie Brachat, and Jun Shi for their help in the course of this study.

We all were Novartis Pharma AG employees at the time of work completion.

S.S. and B.F. conceived and designed the experiments and analyzed the data; A.B., D.S., and S.G. contributed to the design, execution, and analysis of *in vitro* experiments; E.P. and S.M. contributed to the design, execution, and analysis of animal experiments; J.L.-D. analyzed microarray data; E.N., C.D., and C.F. contributed to the data analysis; B.F. supervised the project; and S.S. D.J.G., and B.F. cowrote the manuscript.

REFERENCES

1. Egerman MA, Glass DJ. 2014. Signaling pathways controlling skeletal muscle mass. Crit Rev Biochem Mol Biol 49:59–68. https://doi.org/10.3109/10409238.2013.857291.
2. Stitt TN, Drujan D, Clarke BA, Panaro F, Timofeyva Y, Kline WO, Gonzalez M, Yancopoulos GD, Glass DJ. 2004. The IGF-1/PI3K/Akt pathway prevents expression of muscle atrophy-induced ubiquitin ligases by inhibiting FOXO transcription factors. Mol Cell 14:395–403. https://doi.org/10.1016/S1097-2765(04)00211-4.
3. Sandri M. 2014. Regulation and involvement of the ubiquitin ligases in muscle atrophy. Free Radic Biol Med 75(Suppl 1):S4. https://doi.org/10.1016/j.freeradbiomed.2014.10.833.
4. Rommel C, Bodine SC, Clarke BA, Rossman R, Nunez L, Stitt TN, Yancopoulos GD, Glass DJ. 2001. Mediation of IGF-1-induced skeletal myotube hypertrophy by PI(3)K/Akt/mTOR and PI(3)K/Akt/GSK3 pathways. Nat Cell Biol 3:1009–1013. https://doi.org/10.1038/ncb1101-1009.
5. Babula P, Masarik M, Adam V, Eckschlager T, Stiborova M, Trnkova L, Skutkova H, Provaznik I, Hubalek J, Kizek R. 2012. Mammalian metallothioneins: properties and functions. Metallomics 4:739–750. https://doi.org/10.1039/c2mt20081c.
6. Kimura T, Kambe T. 2016. The functions of metallothionein and ZIP and ZnT transporters: an overview and perspective. Int J Mol Sci 17:336. https://doi.org/10.3390/ijms17030336.
7. Lindeque JZ, Levanets O, Louw R, van der Westhuizen FH. 2010. The involvement of metallothioneins in mitochondrial function and disease. Curr Protein Pept Sci 11:292–309. https://doi.org/10.2174/138920310791233378.

8. Ruttkay-Nedecky B, Nejdl L, Gumulec J, Zitka O, Masarik M, Eckschlager T, Stiborova M, Adam V, Kizek R. 2013. The role of metallothionein in oxidative stress. Int J Mol Sci 14:6044–6066. https://doi.org/10.3390/ijms14036044.
9. Krizkova S, Ryvolova M, Hrabeta J, Adam V, Stiborova M, Eckschlager T, Kizek R. 2012. Metallothioneins and zinc in cancer diagnosis and therapy. Drug Metab Rev 44:287–301. https://doi.org/10.3109/03602532.2012.725414.
10. Mocchegiani E, Costarelli L, Basso A, Giacconi R, Piacenza F, Malavolta M. 2013. Metallothioneins, ageing and cellular senescence: a future therapeutic target. Curr Pharm Des 19:1753–1764. https://doi.org/10.2174/1381612811319090022.
11. Bolognin S, Cozzi B, Zambenedetti P, Zatta P. 2014. Metallothioneins and the central nervous system: from a deregulation in neurodegenerative diseases to the development of new therapeutic approaches. J Alzheimers Dis 41:29–42.
12. Latres E, Amini AR, Amini AA, Griffiths J, Martin FJ, Wei Y, Lin HC, Yancopoulos GD, Glass DJ. 2005. Insulin-like growth factor-1 (IGF-1) inversely regulates atrophy-induced genes via the phosphatidylinositol 3-kinase/Akt/mammalian target of rapamycin (PI3K/Akt/mTOR) pathway. J Biol Chem 280:2737–2744. https://doi.org/10.1074/jbc.M407517200.
13. Lecker SH, Jagoe RT, Gilbert A, Gomes M, Baracos V, Bailey J, Price SR, Mitch WE, Goldberg AL. 2004. Multiple types of skeletal muscle atrophy involve a common program of changes in gene expression. FASEB J 18:39–51. https://doi.org/10.1096/fj.03-0610com.
14. Urso ML, Scrimgeour AG, Chen YW, Thompson PD, Clarkson PM. 2006. Analysis of human skeletal muscle after 48 h immobilization reveals alterations in mRNA and protein for extracellular matrix components. J Appl Physiol (1985) 101:1136–1148. https://doi.org/10.1152/japplphysiol.00180.2006.
15. Hyldahl RD, O'Fallon KS, Schwartz LM, Clarkson PM. 2010. Knockdown of metallothionein 1 and 2 does not affect atrophy or oxidant activity in a novel in vitro model. J Appl Physiol (1985) 109:1515–1523. https://doi.org/10.1152/japplphysiol.00588.2010.
16. DeRuisseau LR, Recca DM, Mogle JA, Zoccolillo M, DeRuisseau KC. 2009. Metallothionein deficiency leads to soleus muscle contractile dysfunction following acute spinal cord injury in mice. Am J Physiol Regul Integr Comp Physiol 297:R1795–R1802. https://doi.org/10.1152/ajpregu.00263.2009.
17. Maret W. 2011. Redox biochemistry of mammalian metallothioneins. J Biol Inorg Chem 16:1079–1086. https://doi.org/10.1007/s00775-011-0800-0.
18. Kambe T, Tsuji T, Hashimoto A, Itsumura N. 2015. The Physiological, biochemical, and molecular roles of zinc transporters in zinc homeostasis and metabolism. Physiol Rev 95:749–784. https://doi.org/10.1152/physrev.00035.2014.
19. Yamasaki S, Sakata-Sogawa K, Hasegawa A, Suzuki T, Kabu K, Sato E, Kurosaki T, Yamashita S, Tokunaga M, Nishida K, Hirano T. 2007. Zinc is a novel intracellular second messenger. J Cell Biol 177:637–645. https://doi.org/10.1083/jcb.200702081.
20. Haase H, Maret W. 2003. Intracellular zinc fluctuations modulate protein tyrosine phosphatase activity in insulin/insulin-like growth factor-1 signaling. Exp Cell Res 291:289–298. https://doi.org/10.1016/S0014-4827(03)00406-3.
21. Lynch CJ, Patson BJ, Goodman SA, Trapolsi D, Kimball SR. 2001. Zinc stimulates the activity of the insulin- and nutrient-regulated protein kinase mTOR. Am J Physiol Endocrinol Metab 281:E25–E34.
22. Bellomo E, Hogstrand C, Maret W. 2014. Redox and zinc signalling pathways converging on protein tyrosine phosphatases. Free Radic Biol Med 75(Suppl 1):S9. https://doi.org/10.1016/j.freeradbiomed.2014.10.851.
23. Mocchegiani E, Giacconi R, Malavolta M. 2008. Zinc signalling and subcellular distribution: emerging targets in type 2 diabetes. Trends Mol Med 14:419–428. https://doi.org/10.1016/j.molmed.2008.08.002.
24. Li Y, Maret W. 2009. Transient fluctuations of intracellular zinc ions in cell proliferation. Exp Cell Res 315:2463–2470. https://doi.org/10.1016/j.yexcr.2009.05.016.
25. Hirano T, Murakami M, Fukada T, Nishida K, Yamasaki S, Suzuki T. 2008. Roles of zinc and zinc signaling in immunity: zinc as an intracellular signaling molecule. Adv Immunol 97:149–176. https://doi.org/10.1016/S0065-2776(08)00003-5.
26. Ibebunjo C, Chick JM, Kendall T, Eash JK, Li C, Zhang Y, Vickers C, Wu Z, Clarke BA, Shi J, Cruz J, Fournier B, Brachat S, Gutzwiller S, Ma Q, Markovits J, Broome M, Steinkrauss M, Skuba E, Galarneau JR, Gygi SP, Glass DJ. 2013. Genomic and proteomic profiling reveals reduced mitochondrial function and disruption of the neuromuscular junction driving rat sarcopenia. Mol Cell Biol 33:194–212. https://doi.org/10.1128/MCB.01036-12.
27. Russell ST, Siren PM, Siren MJ, Tisdale MJ. 2009. Attenuation of skeletal muscle atrophy in cancer cachexia by D-myo-inositol 1,2,6-triphosphate. Cancer Chemother Pharmacol 64:517–527. https://doi.org/10.1007/s00280-008-0899-z.
28. Maret W, Krezel A. 2007. Cellular zinc and redox buffering capacity of metallothionein/thionein in health and disease. Mol Med 13:371–375.
29. Lai KM, Gonzalez M, Poueymirou WT, Kline WO, Na E, Zlotchenko E, Stitt TN, Economides AN, Yancopoulos GD, Glass DJ. 2004. Conditional activation of Akt in adult skeletal muscle induces rapid hypertrophy. Mol Cell Biol 24:9295–9304. https://doi.org/10.1128/MCB.24.21.9295-9304.2004.
30. Masters BA, Kelly EJ, Quaife CJ, Brinster RL, Palmiter RD. 1994. Targeted disruption of metallothionein I and II genes increases sensitivity to cadmium. Proc Natl Acad Sci U S A 91:584–588. https://doi.org/10.1073/pnas.91.2.584.
31. Michalska AE, Choo KH. 1993. Targeting and germ-line transmission of a null mutation at the metallothionein I and II loci in mouse. Proc Natl Acad Sci U S A 90:8088–8092. https://doi.org/10.1073/pnas.90.17.8088.
32. Beattie JH, Wood AM, Newman AM, Bremner I, Choo KH, Michalska AE, Duncan JS, Trayhurn P. 1998. Obesity and hyperleptinemia in metallothionein (-I and -II) null mice. Proc Natl Acad Sci U S A 95:358–363. https://doi.org/10.1073/pnas.95.1.358.
33. Glass DJ. 2010. PI3 kinase regulation of skeletal muscle hypertrophy and atrophy. Curr Top Microbiol Immunol 346:267–278.
34. Basualto-Alarcón C, Jorquera G, Altamirano F, Jaimovich E, Estrada M. 2013. Testosterone signals through mTOR and androgen receptor to induce muscle hypertrophy. Med Sci Sports Exerc 45:1712–1720. https://doi.org/10.1249/MSS.0b013e31828cf5f3.
35. Lee NK, Skinner JP, Zajac JD, MacLean HE. 2011. Ornithine decarboxylase is upregulated by the androgen receptor in skeletal muscle and regulates myoblast proliferation. Am J Physiol Endocrinol Metab 301:E172–E179. https://doi.org/10.1152/ajpendo.00094.2011.
36. Bongers KS, Fox DK, Kunkel SD, Stebounova LV, Murry DJ, Pufall MA, Ebert SM, Dyle MC, Bullard SA, Dierdorff JM, Adams CM. 2015. Spermine oxidase maintains basal skeletal muscle gene expression and fiber size and is strongly repressed by conditions that cause skeletal muscle atrophy. Am J Physiol Endocrinol Metab 308:E144–E158. https://doi.org/10.1152/ajpendo.00472.2014.
37. Bodine SC, Furlow JD. 2015. Glucocorticoids and skeletal muscle. Adv Exp Med Biol 872:145–176. https://doi.org/10.1007/978-1-4939-2895-8_7.
38. Wray CJ, Mammen JM, Hershko DD, Hasselgren PO. 2003. Sepsis upregulates the gene expression of multiple ubiquitin ligases in skeletal muscle. Int J Biochem Cell Biol 35:698–705. https://doi.org/10.1016/S1357-2725(02)00341-2.
39. Falduto MT, Czerwinski SM, Hickson RC. 1990. Glucocorticoid-induced muscle atrophy prevention by exercise in fast-twitch fibers. J Appl Physiol (1985) 69:1058–1062.
40. Applied Biosystems. 2001. ABI user bulletin UB #2: ABI Prism 7700 sequence detection system. Relative quantitation of gene expression. Applied Biosystems, Foster City, CA.
41. Verbanac D, Milin C, Domitrovic R, Giacometti J, Pantovic R, Ciganj Z. 1997. Determination of standard zinc values in the intact tissues of mice by ICP spectrometry. Biol Trace Elem Res 57:91–96.